

Photoionization and ion cyclotron resonance studies of the ion chemistry of ethylene oxide*

Reed R. Corderman, P. R. LeBreton,[†] S. E. Buttrill, Jr.,[‡] A. D. Williamson, and J. L. Beauchamp[§]

Arthur Amos Noyes Laboratory of Chemical Physics, California Institute of Technology, Pasadena, California 91125^{||}

(Received 6 November 1975)

Time-resolved photoionization mass spectrometry (PIMS), ion cyclotron resonance spectroscopy (ICR), and photoelectron spectroscopy have been employed to study the formation of the ethylene oxide molecular ion and its subsequent ion-molecule reactions which lead to the products $C_2H_5O^+$ and $C_3H_5O^+$. Earlier observations that a structurally and energetically modified species $(C_2H_4O^+)^*$ is an intermediate in the production of $C_3H_5O^+$ are confirmed. The PIMS data detail the effects of internal energy on reactivity, with the ratio of $C_3H_5O^+$ to $C_2H_5O^+$ increasing by an order of magnitude with a single quantum of vibrational energy. Evidence is presented for the formation of $(C_2H_4O^+)^*$ in a collision-induced isomerization which yields a ring-opened structure by C-C bond cleavage. This species contains considerable internal excitation which is relaxed in collisions with ethylene oxide or bath gases such as SF_6 prior to reaction. The relaxed ring-opened $C_2H_4O^+$ ion reacts with neutral ethylene oxide by CH_2^+ transfer to yield an intermediate product ion $C_3H_6O^+$ which gives $C_3H_5O^+$ by loss of H. Isotopic product distributions observed in a mixture of ethylene oxide and ethylene oxide- d_4 are consistent with this mechanism. The effects of ion kinetic energy on reactivity are explored using ICR techniques. Increased reactant ion kinetic energy leads to collision-induced dissociation of $C_2H_4O^+$ rather than isomerization to the open form.

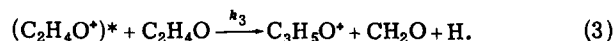
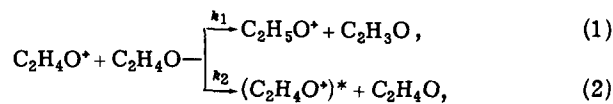
I. INTRODUCTION

Highly strained small ring compounds such as ethylene oxide and cyclopropane are of particular interest since they can rearrange under appropriate conditions to more stable acyclic isomers. The ion chemistry of the smallest heterocyclic oxygen compound, ethylene oxide, has been extensively studied by mass spectrometric¹⁻⁵ and ion cyclotron resonance⁶⁻⁸ (ICR) experiments. Charge localization, predominantly on the oxygen center,⁹ renders the ion-molecule reactions of ethylene oxide less intricate than those of cyclopropane and other small hydrocarbons.¹⁰ Table I shows that both the ethylene oxide radical cation and protonated ethylene oxide are high energy isomers of $C_2H_4O^+$ and $C_2H_5O^+$, respectively, while the lower energy ring opened and acetaldehyde ion structures are from 11 to 35 kcal/mole more stable. Collisional processes may trigger the rearrangement of cyclic $C_2H_4O^+$ and $C_2H_5O^+$, with concomitant energy release to internal modes. The resulting structurally and energetically modified species may have a substantially different reactivity than the precursor.

The structural integrity and differing reactivity of the three $C_2H_5O^+$ isomers VII, VIII, and IX (Table I) has been demonstrated in several previous studies. Beauchamp and Dunbar dealt with the identification of the three ions VII-IX by comparing their ion chemistry.⁶ The similarities in reactivity of VIII and IX did not allow them to be distinguished.⁶ Our recent ICR study of the ion-molecule reactions in mixtures of ethylene oxide with PH_3 or H_2S established the cyclic structure IX of protonated ethylene oxide ions remaining at long ion trapping times or at high pressures.⁸ When ethylene oxide is protonated by H_3^+ , the large reaction exothermicity leads to both fragmentation and rearrangement to the more stable ion VIII.^{5,7}

In comparison to the above studies of $C_2H_5O^+$, the



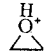
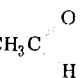
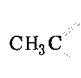
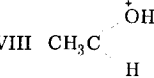

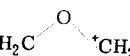
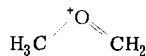
structure and reactivity of the different $C_2H_4O^+$ isomers IV, V, and VI, are not as well characterized. Two product ions, $C_2H_5O^+$ and $C_3H_5O^+$, result from the reaction of $C_2H_4O^+$ with ethylene oxide. The latter product, which was overlooked in a number of early studies of the ion chemistry of ethylene oxide,^{1,2} was first reported by Beauchamp and Dunbar.⁶ Blair and Harrison studied the ion-molecule reactions of ethylene oxide alone, and also in mixtures with $(CD_3)_2O$, $(CH_3)_2CO$, CH_3CHO , and CD_3CDO .⁴ They concluded that while the $C_2H_4O^+$ ion formed initially by electron impact reacts only slowly to form detectable products, it undergoes a rapid collisional modification to a more reactive species, $(C_2H_4O^+)^*$, which is principally responsible for the formation of $C_3H_5O^+$ [Reactions (1)-(3)];



In addition, they observe that $(C_2H_4O^+)^*$ reacts with carbonyl compounds by CH_2^+ addition.⁴ In our ICR study of a mixture of C_2H_4O with PH_3 , the product ion $CH_2PH_3^+$ was observed to be produced at the expense of the $C_3H_5O^+$ normally observed in ethylene oxide alone.⁸ This result also suggests that the reactant species is the structurally or energetically modified ion observed by Blair and Harrison.⁴ A characterization of the $(C_2H_4O^+)^*$ ion and a more complete understanding of the ion chemistry of ethylene oxide is the main focus of this work.

In the present study, the ion chemistry initiated by electron impact in ethylene oxide is re-examined at thermal ion energies using trapped ion ICR techniques.¹¹ Additional ICR experiments have been carried out to

TABLE I. Enthalpies of formation of C_2H_4O , $C_2H_4O^+$, and $C_2H_5O^+$ isomers.^a

| Molecule | ΔH_f | Molecular ion | ΔH_f | Protonated molecule | ΔH_f |
|---|---------------------|--|-------------------|---|---------------|
| I  | -12.58 ± 0.15^b | IV  | 230.9 ± 0.5^c | VII  | 169 ± 1^e |
| II  | -39.72 ± 0.15^b | V  | 196.0 ± 0.5^c | VIII  | 143 ± 1^e |
| III  | 44 ± 3^d | VI  | 201.9 ± 5^d | IX  | 158 ± 1^e |

^aAll values in kcal/mole at 298 °K.^bReference 48.^cReference 19.^dEstimated, see Appendix.^eReference 8.

determine both the effect of ion kinetic energy on reactivity and the possibility that an inert diluent can relax the internal energy and affect the reactivity of the proposed $(C_2H_4O^+)^*$ intermediate. Mixtures of C_2H_4O and C_2D_4O have been examined to verify the mechanism and neutral products of Reactions (1)–(3). More importantly, the greater energy resolution provided by photoionization techniques has been employed to prepare $C_2H_4O^+$ with well-characterized internal energy distributions. Using time-resolved photoionization mass spectrometry,¹² the kinetics of Processes (1)–(3) are measured at selected photon wavelengths. The present study is a continuation of our efforts to understand the effects of internal energy on the reactivity of molecular ions.^{13–15}

Previous photoelectron and photoionization studies have elucidated several features of the molecular and electronic structure of ethylene oxide.^{9,16–20} The ground ionic state of $C_2H_4O^+$ is formed by removal of a $2b_2\pi$ electron largely localized on the oxygen atom.⁹ The first band of the photoelectron spectrum exhibits vibrational structure which is associated with either CH_2 scissoring or symmetric ring breathing modes.^{9,16} In an effort to determine which motion is excited upon photoionization near threshold, the photoelectron spectrum of ethylene oxide- d_4 was recorded. Several previous photoionization studies of ethylene oxide^{19,20} and acetaldehyde^{19,21} are useful for interpreting the present results.

II. EXPERIMENTAL

The Caltech–Jet propulsion laboratory photoionization mass spectrometer used in this study has been described in detail elsewhere.^{12–15,22} Briefly, the instrument consists of a differentially pumped windowless Hinteregger lamp mounted on a 1-m normal incidence monochromator (McPherson model 225). Ions are removed from the differentially pumped ionization chamber using a shaped repeller and extraction lens assembly designed for efficient collection of ions at relatively low repeller voltages and after correspondingly long residence times in the source. Ions are mass analyzed with a quadrupole mass filter (Extranuclear 324-9) and detected with a Channeltron multiplier using conven-

tional ion counting techniques. A cooled photomultiplier with a coating of sodium salicylate monitors the intensity of the light passing through the ion source. Over the wavelength region scanned, the relative quantum efficiency of the scintillator was assumed constant.²³

For the time resolved photoionization mass spectrometry experiments,¹² a pulsed light source is required, so the dc power supply was replaced by a Cober high power pulse generator model 605P with a P27 pulse generator plug in. The output pulse width was 10 μ sec and the pulse rate was 350 Hz. In order to record the distribution of ion arrival times, the amplified output pulses from the Channeltron were routed to a Nuclear Data multichannel analyzer. The time resolution was limited by the 10 μ sec per channel minimum dwell time of the analyzer. The experimental repetition rate was limited by the 2.6 msec required to scan through the smallest memory block of 256 channels. The ion arrival time distribution was accumulated for 10^5 lamp pulses.

A MgF_2 coated grating blazed at 1200 Å and ruled with 1200 lines mm^{-1} was used in first order in the present experiments. The ionization chamber pressure was measured with a model 90 H1 MKS Baratron capacitance manometer. Other pertinent operating conditions include: source temperature, ambient (20–25 °C); sample pressure, 8×10^{-4} torr; resolution, 1.4 Å; repeller field, 0.1 V cm^{-1} ; ion energy for mass analysis, 10.0 eV. The hydrogen–many line spectrum was utilized in the wavelength range examined.

Ion cyclotron resonance (ICR) experiments performed in conjunction with the present study employed an instrument built at Caltech equipped with an electromagnet capable of a maximum field strength of 23.5 kG. The instrumentation and experimental techniques have been previously discussed in detail.^{11,24,25} The effects of translational energy on the reactions of ethylene oxide were performed by applying a constant rf electric field at the cyclotron frequency of the reactant ion to the source region of the ICR cell. Before entering the analyzer region of the cell, reactant ions are accelerated to an average energy given in Eq. (4),

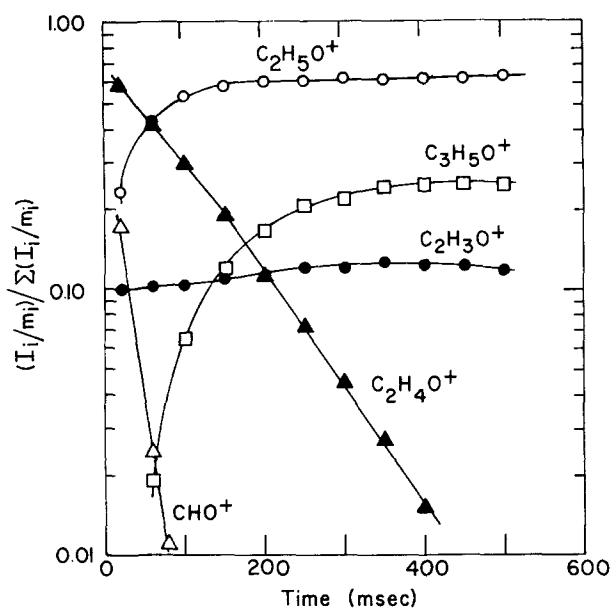


FIG. 1. ICR results for temporal variation of ion abundance in ethylene oxide at 1.5×10^{-6} torr following a 14 eV, 10 msec electron beam pulse.

$$T = e^2 E_2^2 \tau_s^2 / 8m, \quad (4)$$

where E_2 is the amplitude of the irradiating rf electric field and τ_s is the time the ions spend in the source region.²⁸ All ICR experiments were done at ambient temperature (20–25 °C).

Photoelectron spectra were obtained using a photoelectron spectrometer built at Caltech employing a He(I) resonance lamp and a cylindrical 127° electrostatic analyzer of standard design.⁹ The analyzer potentials can be adjusted to give a maximum resolution of about 17 millielectron volts (meV), however in these studies the resolution was maintained at 25 meV. The spectra were calibrated with the $^2P_{1/2}$ and $^2P_{3/2}$ lines of Ar both before and after scanning the sample spectrum to insure that experimental conditions remained constant. All spectra were recorded at ambient temperature (20–25 °C).

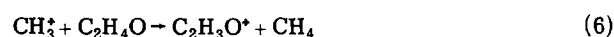
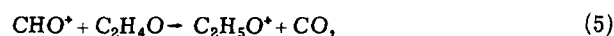
The ethylene oxide and sulphur hexafluoride used in this study were obtained from commercial sources and

were not further purified. Ethylene oxide- d_4 was obtained from Merck, Sharp, and Dohme of Canada, Ltd. and purified by gas chromatography. Before use, each sample was degassed by several freeze-pump-thaw cycles.

III. RESULTS

A. ICR study of C_2H_4O

The 70 eV ICR mass spectrum of ethylene oxide at 2.5×10^{-7} torr is in good agreement with the previously published spectra.^{27–29} At 14 eV the major ions observed and their relative abundances are $C_2H_4O^+$ (53%), $C_2H_3O^+$ (8%), CHO^+ (32%), and CH_3^+ (3%). While the ion chemistry of ethylene oxide has been investigated using both ICR⁶ and low energy electron beam trapping techniques,⁴ the trapped-ion ICR mass spectrum at thermal ion energies has not been previously reported. The temporal variation of relative ion abundance following a 14 eV, 10 msec electron beam pulse at 1.5×10^{-6} torr is shown in Fig. 1.³⁰ Reactions of the parent ion lead to the formation of $C_2H_5O^+$ and $C_3H_5O^+$, Processes (1)–(3). After accounting for other contributions to $C_2H_5O^+$, the data in Fig. 1 indicates that the ratio of $C_2H_5O^+$ to $C_3H_5O^+$ changes with time in a manner consistent with the proposed scheme of bimolecular Reactions (1)–(3). The relative abundance of the $C_2H_4O^+$ ion does not decrease in an exponential fashion expected for a pseudo first-order reaction scheme, but rather more slowly before ~150 msec and faster thereafter. Termolecular reactions are ruled out by the low pressure of the ICR experiment, 1.5×10^{-6} torr, and by the similarity of our observations to those of Blair and Harrison at 3.6×10^{-4} torr, some 240 times greater pressure.⁴ The CHO^+ fragment ion reacts by fast proton transfer to neutral ethylene oxide [Reaction (5)]. The $C_2H_3O^+$ fragment ion is unreactive; this ion is also produced from hydride abstraction of C_2H_4O by CH_3^+ [Reaction (6)] which is



present in low abundance at 14 eV. From the slopes of the lines in Fig. 1 and the known pressure of C_2H_4O , the total apparent rate constants observed for Reactions (1)–(3), and (5) are summarized in Table II. The

TABLE II. Ion-molecule reactions, rate constants, and reaction enthalpies in ethylene oxide.

| Reaction | k^a | | ΔH^b |
|---|-------------------|--|--------------------------------|
| | This work | Literature (Ref.) | |
| $CHO^+ + C_2H_4O \rightarrow C_2H_5O^+ + CO$ | 1.3 ± 0.1 | $1.65 \pm 0.3(4)$ $1.75 \pm 0.2(1)$ | -40.4 ± 2 |
| $C_2H_4O^+ + C_2H_4O \rightarrow \left\{ \begin{array}{l} C_2H_5O^+ + C_2H_3O \\ C_3H_5O^+ + CH_2O + H \end{array} \right.$ | 0.19 ± 0.02^c | $0.15 \pm 0.03(4)$ $0.2 \pm 0.1(2)$ | -18.3 ± 3 -41.2 ± 3 |
| $CH_3^+ + C_2H_4O \rightarrow C_2H_3O^+ + CH_4$ | ... | ... | -62.3 ± 2 |

^a All rate constants in units of $10^{-9} \text{ cm}^3 \text{ molecule}^{-1} \cdot \text{sec}^{-1}$.

^b All values in kcal/mole. See Appendix for heats of formation used in this study.

^c Limiting slope at long times (see text).

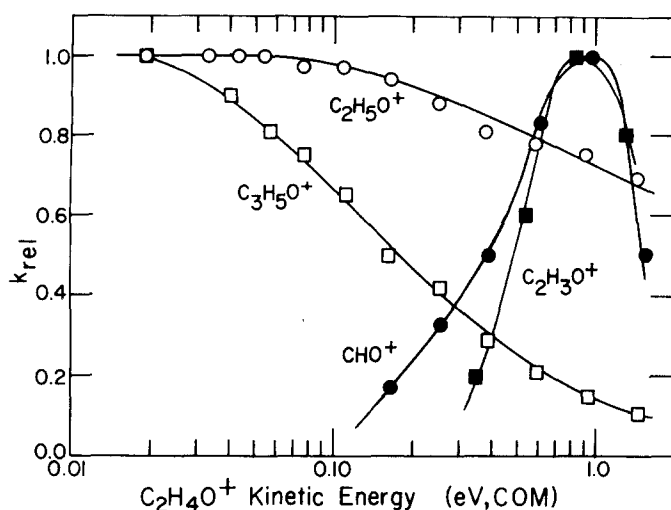


FIG. 2. ICR results for the variation with relative kinetic energy of the product yields for reactions of $C_2H_4O^+$ with C_2H_4O . The data for $C_2H_5O^+$ and $C_3H_5O^+$ are normalized relative to their thermal rate constants; the data for CHO^+ and $C_2H_3O^+$ are normalized to unity at their maximum abundance (see text).

Langevin, or collision rate constant^{31,32} is calculated to be $1.0 \times 10^{-9} \text{ cm}^3 \text{ molecule}^{-1} \text{ sec}^{-1}$, an order of magnitude larger than the observed rate constants. Theories which include the effect of the permanent dipole moment predict rates even larger.³³⁻³⁵

At higher pressures ($\geq 10^{-4}$ torr), additional product ions are observed in the 14 eV ICR single resonance spectrum of ethylene oxide. The minor product ion $C_3H_6O^+$ is discussed further below. The $C_2H_3O^+$ and $C_2H_5O^+$ ions are observed to cluster with neutral ethylene oxide. In agreement with earlier work, the proton bound dimer, $(C_2H_4O)_2H^+$, is observed to eliminate H_2O to form a small amount of $C_4H_7O^+$.⁴

B. Effects of ion kinetic energy on the reactivity of $C_2H_4O^+$

The effects of translational energy on the reactions of $C_2H_4O^+$ with neutral ethylene oxide were investigated using the continuous rf irradiation method developed by Buttrill.²⁶ The kinetic energy dependence of the relative rates of reactions 1-3 is shown in Fig. 2. Quantitative comparison of the change in reaction rate is difficult because of the different reaction orders for the production of $C_2H_5O^+$ and $C_3H_5O^+$. At kinetic energies in excess of 0.1 eV, collision induced dissociation of the $C_2H_4O^+$ ion to give both CHO^+ and $C_2H_3O^+$ is observed [Reactions (7) and (8)];

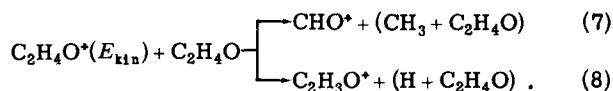
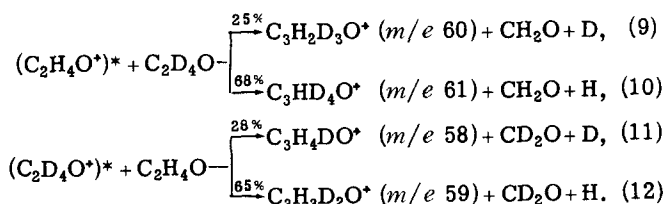


Figure 2 illustrates that the relative reaction rates for product formation, Reactions (1)-(3), decrease while those for collision induced dissociation increase as the kinetic energy of $C_2H_4O^+$ is varied from thermal energies to ~ 2 eV. At their maxima the products CHO^+ , $C_2H_3O^+$, and $C_3H_5O^+$ are 10%, 5%, and 10%, respectively, of the $C_2H_5O^+$ abundance

at the energy. While the neutral products in Reactions (7) and (8) are uncertain, the use of SF_6 diluent gas provided similar results consistent with a process whereby collisional activation is followed by unimolecular dissociation to yield the observed products. For a given translational energy, the $C_2H_5O^+$ yield decreases relatively more than the $C_2H_3O^+$ yield. This suggests that the structure of energetically modified $(C_2H_4O^+)^*$ ion [Eq. (2)] is collisionally dissociated more readily than the intact $C_2H_4O^+$ ion. A previous tandem mass spectrometric study of the collision induced dissociation of the $C_2H_4O^+$ ion scattered from He atoms reported a threshold of 0.9 ± 0.2 eV for the appearance of CHO^+ ,³⁶ in poor agreement with our result of ~ 0.1 eV.

C. Mixtures of C_2H_4O and C_2D_4O

Examination of a 1:1 mixture of C_2H_4O with C_2D_4O reveals information about the mechanism of formation of the product ions $C_2H_5O^+$ and $C_3H_5O^+$. Double resonance^{24,25} confirms that the protonated parent ion, $C_2H_5O^+$, is produced both by proton transfer and hydrogen atom abstraction. The relative extent of proton transfer is approximately three times that of hydrogen atom abstraction. Double resonance also demonstrates that the extent of charge transfer between the isotopic molecular ions is negligible compared to the other reaction channels at thermal energies. Both drift-mode and trapped-ion mass spectra of C_2H_4O with C_2D_4O give an equivalent distribution of $C_3H_5-nD_nO^+$ ($n=0-5$) product ions. Ion ejection experiments yield the product distributions for the cross Reactions (9)-(12) occurring in this mixture³⁷;



The observed product distribution suggests a specific mechanism for the formation of the $C_3H_5O^+$ product ion which is in accordance with the reaction scheme of Eqs. (1)-(3). The structurally or energetically modified $(C_2H_4O^+)^*$ reacts with ethylene oxide- d_4 by CH_2^+ transfer to produce $C_3H_2D_4O^+$. This ion subsequently loses D or H by unimolecular decomposition giving the observed product ions $C_3H_2D_3O^+$ and $C_3HD_4O^+$, Eqs. (9) and (10). A similar scheme for the reaction of $(C_2D_4O^+)^*$ with C_2H_4O via the intermediate product ion $C_3H_4D_2O^+$ is also observed, Eqs. (11) and (12). The observed product distribution is considered in greater detail below.

D. Effects of added diluent gas on $C_2H_4O^+$ reactivity

Further evidence in support of a structurally or energetically modified intermediate ion $(C_2H_4O^+)^*$ responsible for the production of $C_3H_5O^+$ [Reactions (2) and (3)] was obtained from the effect of added SF_6 gas on the high pressure ICR mass spectrum of ethylene oxide. Studies were conducted at electron energies below the first ionization potential of the diluent.^{9,38} A recent investigation of the collisional deactivation of

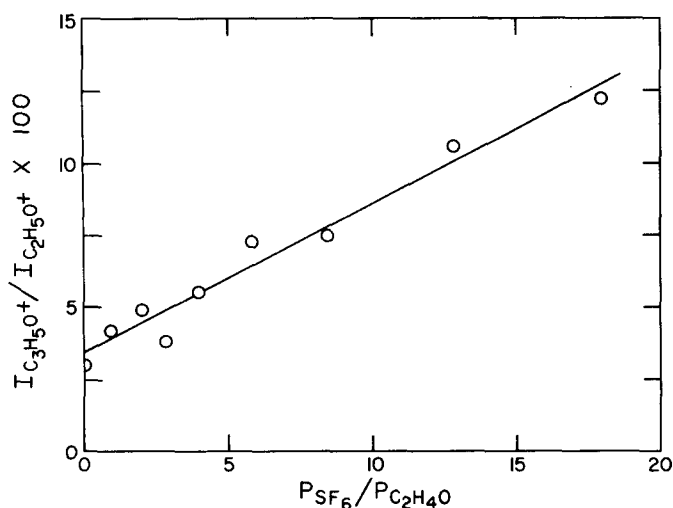


FIG. 3. Enhancement of $C_3H_5O^+$ relative to $C_2H_5O^+$ as SF_6 pressure is increased at 14 eV and 1.2×10^{-5} torr ethylene oxide.

$(C_2H_5O^+)^*$ using a variety of monatomic, diatomic, and polyatomic species demonstrated that SF_6 is quite efficient in deactivating vibrationally excited ions,³⁹ and accounts for the choice of SF_6 in this study. At an ethylene oxide pressure of 1.2×10^{-5} torr and an electron energy of 14 eV, the ratio of $C_3H_5O^+$ [produced in the sequence of Reactions (2) and (3)] to $C_2H_5O^+$ [formed in Reaction (1)] increases from 0.03 to 0.12 as the partial pressure of SF_6 is increased from 0 to 2.1×10^{-4} torr (Fig. 3). Under these conditions the extent of conversion to products increases from 28% to 35%. While this increase can be largely attributed to the increased yield of $C_3H_5O^+$ at higher SF_6 pressures, the extent of conversion is difficult to determine accurately due to the effect of collision broadening on the absorption intensities.²⁴ In trapped-ion experiments, where Reactions (1)–(3) have proceeded to completion at long times, the effect of added SF_6 on the product ratio is much smaller. At 8.6×10^{-7} torr of ethylene oxide and 400 msec ion trapping time, corresponding to 99% extent of reaction, the ratio of $C_3H_5O^+$ to $C_2H_5O^+$ changes from 0.57 to 0.80 as the pressure of SF_6 is increased from 0 to 6.7×10^{-6} torr. The contribution of Reaction (5) to the $C_2H_5O^+$ ion abundance is excluded in calculating the product ratio in both experiments. No condensation product ions resulted from interaction of ions derived from ethylene oxide with SF_6 .

E. Photoelectron spectrum of C_2H_4O and C_2D_4O

To interpret the effects of internal excitation on reactivity and to examine the energetics associated with the formation of the various $C_2H_4O^+$ ion states, it is of interest to examine the vibronic structure of the ethylene oxide molecular ion using He(I) photoelectron spectroscopy (PES). The photoelectron spectrum of ethylene oxide has been recorded and discussed in several previous studies.^{9,16,17} The first band, with a vertical ionization potential (I.P.) of 10.560 ± 0.025 eV, originates from the photoionization of an electron from the nonbonding $2b_2\pi$ molecular orbital¹⁶ and exhibits a vibrational spacing of 1150 ± 100 cm^{-1} . This vibrational

structure may be assigned to either the ν_2 totally symmetric CH_2 scissoring mode (1497.5 cm^{-1} in the neutral⁴⁰) or the ν_3 totally symmetric ring breathing mode (1270.5 cm^{-1} in the neutral⁴⁰). In an effort to determine the correct assignment of this vibration, the photoelectron spectrum of ethylene oxide- d_4 was recorded. Figure 4 presents the spectra of both C_2H_4O and C_2D_4O for comparison. Table III gives the observed ionization potentials and Table IV the vibrational sequences for the respective cations and neutrals. The first band of the photoelectron spectrum of C_2D_4O differs from that of C_2H_4O in two respects. The vertical I.P. moves from the (0–0) transition in C_2H_4O to the (0–1) transition in C_2D_4O , reflecting a change in the Franck–Condon factors for the ionization process. The vibrational spacing in the first band changes from 1150 ± 100 cm^{-1} in C_2H_4O to 895 ± 100 cm^{-1} in C_2D_4O , or about 20%. Unfortunately, this shift does not permit the assignment of the vibration to either ν_2 or ν_3 as the frequencies of these two motions both decrease by approximately 20% on going from C_2H_4O to C_2D_4O in the neutral molecules (Table III).⁴¹ Either both modes are excited upon ionization as they are relatively close in energy and belong to the same symmetry class (A_1 in C_{2v} symmetry) or one mode is excited upon ionization and the vibrational energy is partitioned to both.

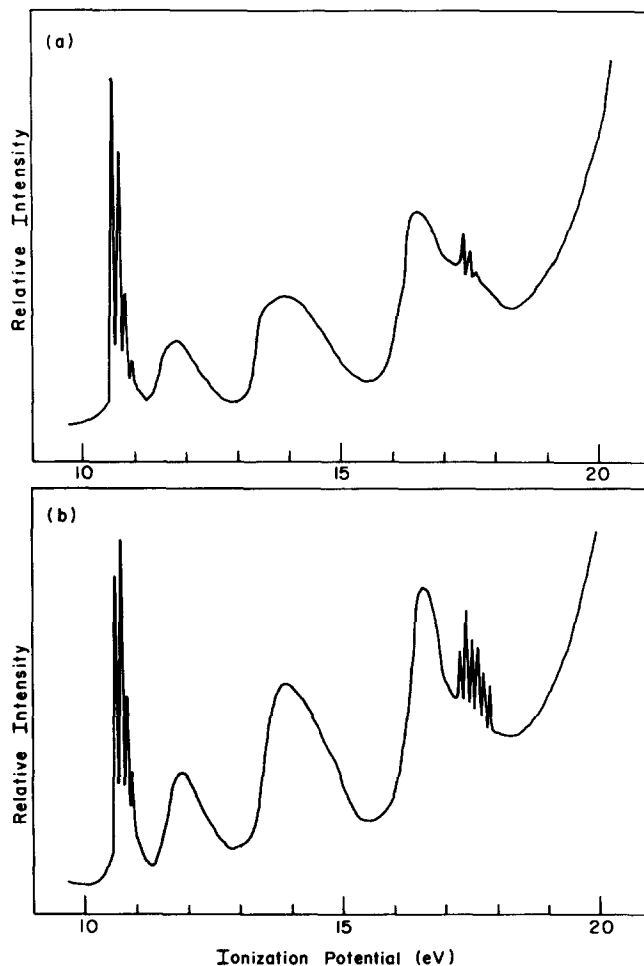


FIG. 4. He(I) photoelectron spectra of ethylene oxide (a) and ethylene oxide- d_4 (b).

TABLE III. Ionization potentials and vibrational series in C_2H_4O and C_2D_4O .

| Molecule | Method | First I. P. | | IP ^a | Vibrational structure | | Second I. P. | |
|-----------|--------|--------------------------|---|-----------------|------------------------|--|------------------------|-----------------------|
| | | This work ^a | Literature ^b | | This work ^c | Literature | This work ^d | Literature |
| C_2H_4O | PES | 10.560 - A, V | 10.56 - A, V ^e | 10.560 | 1156 cm^{-1} | 1120 cm^{-1} ^e 1130 cm^{-1} ^g | 11.84 - V | 11.7 - V ^e |
| | | | | 10.702 | | | | |
| | | | | 10.846 | | | | |
| | | | | 10.988 | | | | |
| C_2H_4O | PIMS | 10.558 ± 0.01 - A | 10.56 - A ^h 10.565 - A ^f | 10.558 | 1100 ± 80 cm^{-1} | 1170 cm^{-1} ^h 1150 cm^{-1} ^f | | |
| | | | | 10.694 | | | | |
| C_2D_4O | PES | 10.571 - A 10.686 - V | | 10.571 | 893 cm^{-1} | | 11.85 - V | |
| | | | | 10.686 | | | | |
| | | | | 10.793 | | | | |
| | | | | 10.903 | | | | |

^aAll values in eV, ±0.025 eV unless otherwise indicated; A = adiabatic, V = vertical.

^bAll values in eV.

^cAll values ±100 cm^{-1} unless otherwise indicated.

^dAll values in eV, ±0.05 eV.

^eReference 16.

^fReference 20.

^gReference 9.

^hReference 19.

The diffuse second band of the photoelectron spectrum of both C_2H_4O (11.84 ± 0.05 eV, vertical I. P.) and C_2D_4O (11.85 ± 0.05 eV, vertical I. P.) results from ionization of the $6a_1\sigma$ molecular orbital.¹⁶ While the first band originates from an orbital largely localized on oxygen, the $6a_1\sigma$ orbital is distributed almost equally over the σ orbitals of the entire molecule.¹⁶ The broad width of the band in the photoelectron spectrum suggests that considerable geometry change is involved in this ionization. Recent photoionization studies show that the threshold for Processes (13) and (14) occur within the second band at 11.54 ± 0.03 and 11.62 ± 0.05 eV,



respectively.¹⁹ These fragmentations may also contribute to the diffuse nature of this photoelectron band.

The third and higher bands are undoubtedly associated

with C-C, C-O, and C-H ionizations.¹⁸ The vibrational progression at 17.5 eV in C_2H_4O is much better resolved into six components in C_2D_4O , and is found to have a spacing of 920 ± 100 cm^{-1} . This spacing is in excellent agreement with the 900 cm^{-1} spacing observed in the 16.5 eV $3a_1'$ cyclopropane- d_6 ^{30,42} band, and suggests a similar type of ionization in C_2D_4O .

F. Photoionization studies

Figure 5 presents photoionization efficiency (PIE) data for $C_2H_4O^+$ between 1190 and 900 Å. Measurements were taken at 5 Å intervals and at low conversion to products. The main features of the $C_2H_4O^+$ data, including the ionization threshold at 10.56 eV, and the continuous rise in the photoionization efficiency from threshold to 13.5 eV, are in agreement with previously reported results.¹⁹ A slight rise at 12.0 eV corresponds to the vertical ionization potential of the $6a_1\sigma$ second band in the photoelectron spectrum of ethylene oxide [Fig. 4(a)]. At the threshold for the $3b_1\sigma$ state, which appears at 13.2 eV in the photoelectron spectrum of ethylene oxide,¹⁶ a break occurs in the PIE curve. For wavelengths near the ionization threshold of ethylene

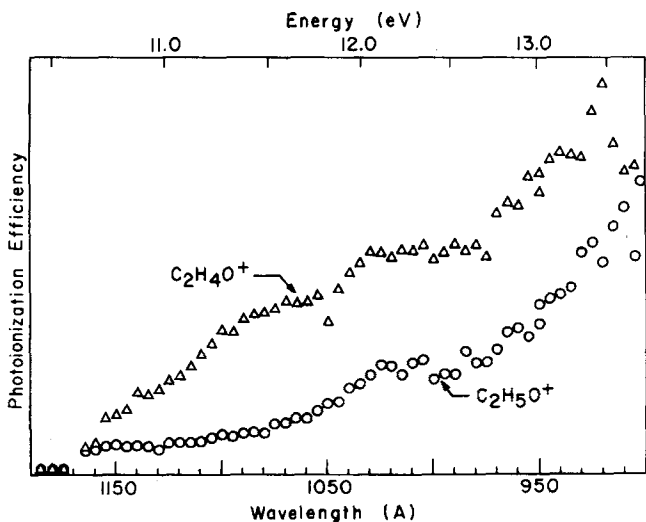


FIG. 5. Apparent photoionization efficiency curves for $C_2H_4O^+$ and $C_2H_5O^+$ normalized at 1166 Å. Data were taken at 5 Å intervals with the hydrogen many-line spectrum from 1190–900 Å.

TABLE IV. Vibrational frequencies of C_2H_4O and C_2D_4O .^a

| Molecule | Neutral | | Cation |
|-----------|-----------------------------------|-------------------------|-------------------|
| | ν_2 -CH ₂ scissors | ν_3 -ring breathing | |
| C_2H_4O | 1495 ^b | 1263 ^b | 1156 ^e |
| | 1490 ^c | 1266 ^c | 1120 ^f |
| | 1497, 5 ^d | 1270, 5 ^d | 1130 ^g |
| C_2D_4O | 1301 ^c | 1013 ^c | 893 ^e |

^aAll values in cm^{-1} .

^bG. Herzberg, *Molecular Spectra and Molecular Structure* (Van Nostrand, New York, 1945), Vol. II, p. 341.

^cReference 41.

^dReference 40.

^eThis work, all values ±100 cm^{-1} .

^fReference 9.

^gReference 16.

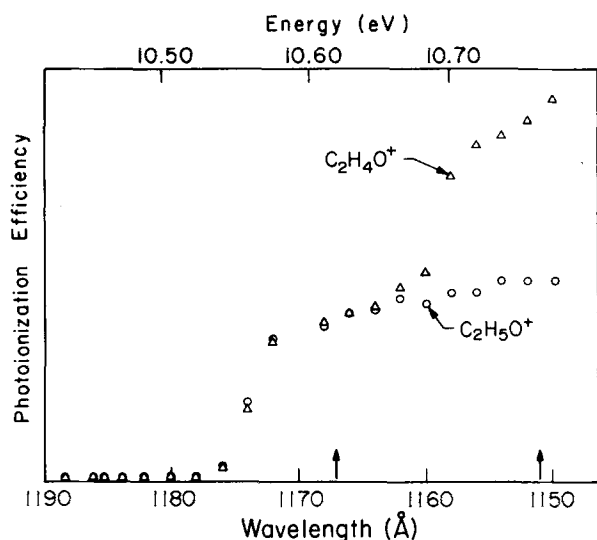


FIG. 6. Apparent photoionization efficiency curves for $C_2H_4O^+$ and $C_2H_5O^+$ normalized at 1166 Å in the energy region 10.4 to 10.8 eV recorded at low conversion and 2 Å intervals. Arrows indicate photon energies used to produce $C_2H_4O^+$ in the $v=0$ (1167 Å) and distribution of $v=0$ and $v=1$ (1151 Å) vibrational levels. The separation of the two sets of data below 1162 Å indicates a decrease in the rate of production of $C_2H_5O^+$ with increasing $C_2H_4O^+$ vibrational energy.

oxide where prominent vibrational structure is observed, measurements were taken at 2 Å intervals, Fig. 6. From the step heights, the relative Franck-Condon factors for ionization into the $v=0$ and $v=1$ vibrational levels of the $C_2H_4O^+$ molecular ion at 1151 Å are calculated to be 0.57 and 0.43, respectively. These results are in excellent agreement with the Franck-Condon factors obtained from the He(I) photoelectron spectrum of C_2H_4O , Table V. The agreement between the Franck-Condon factors for threshold ionization and those for He(I) ionization, combined with the absence of pronounced autoionization features near threshold, suggests that $C_2H_4O^+$ is produced predominantly by direct ionization.

Included in Figs. 5 and 6 is the photoionization efficiency curve for $C_2H_5O^+$. The curve is normalized to the $C_2H_4O^+$ curve at 1166 Å on the step associated with ionization into the $v=0$ state of $C_2H_4O^+$. It is apparent comparing the two curves that the $v=1$ level of $C_2H_4O^+$ does not react appreciably to yield $C_2H_5O^+$.

TABLE V. Relative Franck-Condon factors for the excitation of the $v=0$ and $v=1$ states in $C_2H_4O^+$.

| Method | $v=0$ | $v=1$ | Ref. |
|-------------------|-------|-------|-----------|
| PES ^a | 0.56 | 0.44 | This work |
| PES ^a | 0.57 | 0.43 | Ref. 9 |
| PIMS ^b | 0.57 | 0.43 | This work |

^a He(I) 21.21 eV measurements taken from photoelectron spectra.

^b Threshold measurements taken from step heights in photoionization efficiency curve, Fig. 6.

In fact, the photoionization efficiency of $C_2H_5O^+$ stays relatively constant to 1080 Å. At shorter wavelengths, the reactions of fragment ions, principally CHO^+ , become important in producing $C_2H_5O^+$, and the PIE of $C_2H_5O^+$ increases.

The $C_3H_5O^+$ ion was not observed in the PIMS experiment at low conversion. This is consistent with the $C_3H_5O^+$ ion being the product of consecutive bimolecular collisions, in agreement with the ICR results.

The data in Fig. 6 suggest that the $v=1$ state is unreactive in producing $C_2H_5O^+$ in a single collision. To investigate the results of several collisions and to observe the higher order product $C_3H_5O^+$, the time-resolved photoionization mass spectrometry of ethylene oxide near threshold was studied. Figure 7 shows the temporal variation of relative ion abundance for $C_2H_4O^+$ in the $v=0$ (1167 Å) and a mixture of $v=0$ and $v=1$ (1151 Å) states at 8×10^{-4} torr following a 10 μsec light pulse. The arrows in Fig. 6 indicate the photon energies used in the time-resolved PIMS experiment. The relative abundances of the three ions $C_2H_4O^+$, $C_2H_5O^+$, and $C_3H_5O^+$ at long reaction times in the 1167 Å differ markedly from those at 1151 Å, although the difference in photon energies is only 0.150 eV. At 200 μsec, the relative abundance of $C_2H_4O^+$ changes from 5.5% to 28%, $C_2H_5O^+$ from 85% to 56%, and $C_3H_5O^+$ from 8% to 18%, in going from 1167 to 1151 Å. From the relative populations of $v=0$ and $v=1$ ions at 1151 Å (Table V), the temporal variation of relative ion abundance starting with $C_2H_4O^+$ in the $v=1$ vibrational level only may be derived from the data in Fig. 7. Figure 8 presents the $v=1$ time-resolved ion abundances. Two features are apparent:

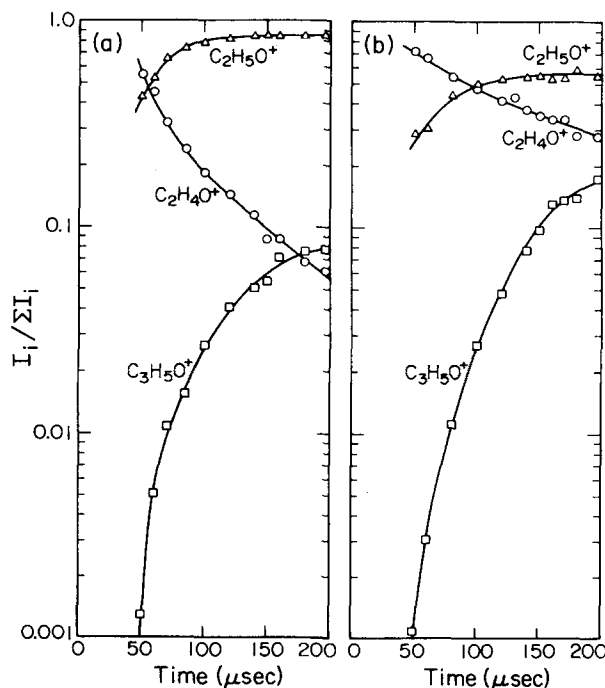


FIG. 7. PIMS results for temporal variation of ion abundance in ethylene oxide at 8×10^{-4} torr following a 10 μsec lamp pulse. $C_2H_4O^+$ ions are prepared initially in the $v=0$, 1167 Å (a) and a mixture of $v=0$ and $v=1$, 1151 Å (b) vibrational levels.

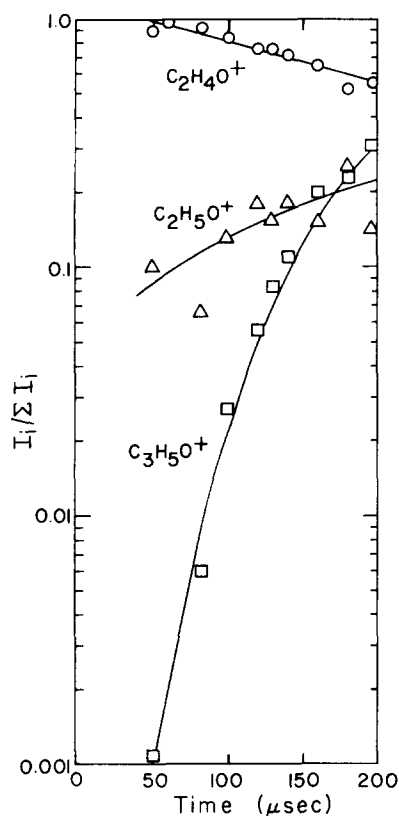
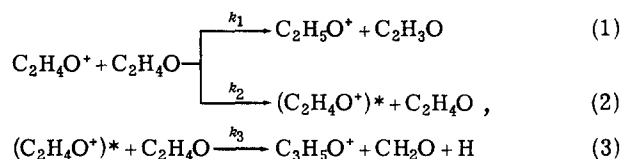


FIG. 8. Calculated temporal variation of ion abundance in ethylene oxide at 8×10^{-4} torr following a $10 \mu\text{sec}$ lamp pulse. $\text{C}_2\text{H}_4\text{O}^+$ ions are prepared initially in the $v=1$ state by subtracting the contribution from the relative population of $\text{C}_2\text{H}_4\text{O}^+$ ions in the $v=0$ vibrational level from the 1151 \AA spectrum [Fig. 7(b)].

The relative abundance of $\text{C}_3\text{H}_5\text{O}^+$ actually becomes greater than that of $\text{C}_2\text{H}_5\text{O}^+$; and the initial slope for the decrease of $\text{C}_2\text{H}_4\text{O}^+$ is much less than observed for the $v=0$ state, Fig. 7(a), indicating that the total reactivity has decreased. Further increases in the relative abundance of $\text{C}_3\text{H}_5\text{O}^+$ are observed when higher vibrational levels are included in the initial distribution.

Data analysis

The data of Figs. 7 and 8 permit a quantitative analysis of the proposed reaction scheme [Eq. (1)–(3)] and allow values for k_1 , k_2 , and k_3 to be extracted. The rate constant k_3 incorporates both the



rate of Reaction (3) and the possible vibrational deactivation of the intermediate $(\text{C}_2\text{H}_4\text{O}^+)^*$ ion by successive collisions with $\text{C}_2\text{H}_4\text{O}$. The protonation of $\text{C}_2\text{H}_4\text{O}$ by $(\text{C}_2\text{H}_4\text{O}^+)^*$, which is probably a minor process, is not considered in the proposed scheme. The time scales of Figs. 7 and 8 were corrected to the actual reaction time by subtracting the ion flight times of approximately $30 \mu\text{sec}$.^{12,22}

Expressions for the relative ionic abundances as a function of k_1 , k_2 , k_3 , and time for Reactions (1)–(3) were derived and fit to the data of Figs. 7 and 8. The results of these calculations are presented in Table VI. For the $v=0$ (1167 \AA) data [Fig. 7(a)], the exponential rise in $\text{C}_2\text{H}_5\text{O}^+$ gives $k_1 + k_2$. From the abundances of $\text{C}_2\text{H}_5\text{O}^+$ and $\text{C}_3\text{H}_5\text{O}^+$ at long reaction times, the ratio k_1/k_2 may be obtained. With both the sum and the ratio of k_1 and k_2 , the individual rate constants were calculated. A value of k_3 was then chosen to fit the observed abundance of $\text{C}_3\text{H}_5\text{O}^+$. A similar procedure was applied to the data in a mixture of $v=0$ and $v=1$ vibrational levels measured at 1151 \AA [Fig. 7(b)]. The abundance of $\text{C}_2\text{H}_5\text{O}^+$ ions produced from $v=1$ state $\text{C}_2\text{H}_4\text{O}^+$ was obtained by subtracting the contribution of $v=0$ state $\text{C}_2\text{H}_4\text{O}^+$ from the total $\text{C}_2\text{H}_5\text{O}^+$ abundance at long reaction times. The abundance of $\text{C}_2\text{H}_5\text{O}^+$ at long reaction times produced from $v=1$ state $\text{C}_2\text{H}_4\text{O}^+$ gives the ratio k_1/k_2 for $v=1$ state $\text{C}_2\text{H}_4\text{O}^+$. The assumption was made that $k_3(v=0)$ equals $k_3(v=1)$. Finally, the total rate constant for the decrease of $\text{C}_2\text{H}_4\text{O}^+$, $k_1 + k_2$, was adjusted until the calculated ion abundances fit the experimental data of Fig. 8.

IV. DISCUSSION

The present results confirm the observations of Blair and Harrison that a structurally or energetically modified species $(\text{C}_2\text{H}_4\text{O}^+)^*$ is an intermediate in the production of $\text{C}_3\text{H}_5\text{O}^+$.⁴ It is apparent from the PIMS data that the formation of $(\text{C}_2\text{H}_4\text{O}^+)^*$ is promoted by internal excitation in the form of vibrational energy. However both the ICR and PIMS data indicate that vibrational excitation alone is not sufficient for the production of $\text{C}_3\text{H}_5\text{O}^+$. We suggest that upon collision ethylene oxide ring opens by C–C bond cleavage producing the

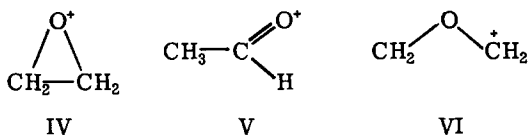
TABLE VI. Observed rate constants from time-resolved photoionization data.

| Process | $k^a(v=0)$ | Prod. dist. ^b | $k^a(v=1)$ | Prod. dist. ^b |
|---|---------------|--------------------------|-----------------|--------------------------|
| $\text{C}_2\text{H}_4\text{O}^+ + \text{C}_2\text{H}_4\text{O} \xrightarrow{k_1} \text{C}_2\text{H}_5\text{O}^+ + \text{C}_2\text{H}_3\text{O}$ | 8.5 ± 0.7 | 0.87 | 0.65 ± 0.25 | 0.24 |
| $\text{C}_2\text{H}_4\text{O}^+ + \text{C}_2\text{H}_4\text{O} \xrightarrow{k_2} (\text{C}_2\text{H}_4\text{O}^+)^* + \text{C}_2\text{H}_4\text{O}$ | 1.3 ± 0.1 | | 2.1 ± 0.3 | |
| $(\text{C}_2\text{H}_4\text{O}^+)^* + \text{C}_2\text{H}_4\text{O} \xrightarrow{k_3} \text{C}_3\text{H}_5\text{O}^+ + \text{CH}_2\text{O} + \text{H}$ | 2.8 ± 0.1 | 0.13 | 2.8 ± 0.1 | 0.76 |

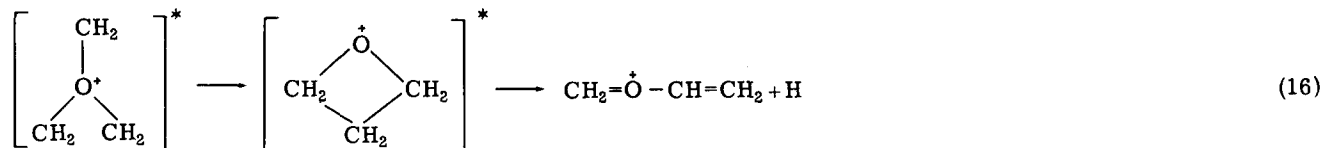
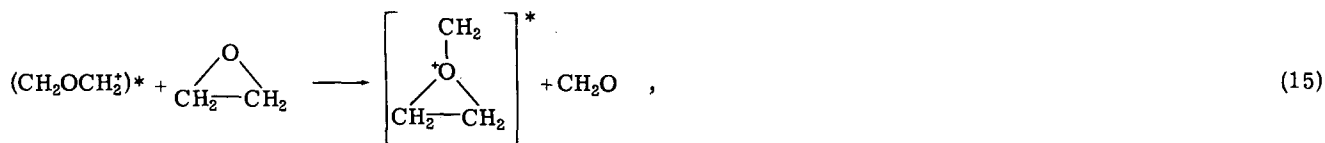
^a All rate constants in units of $10^{-10} \text{ cm}^3 \text{ molecule}^{-1} \cdot \text{sec}^{-1}$.

^b Product distributions at long time, normalized to unity.

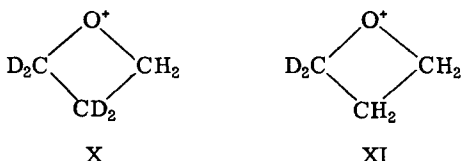
acyclic ion of structure VI (Table I). The



ring opening of cyclic $C_2H_4O^+$ in the $\nu=0$ vibrational



transfer to neutral ethylene oxide. The activated intermediate product ion ($C_3H_5O^+$)*, eliminates H by unimolecular decomposition and ring opens to the more stable acyclic $C_3H_5O^+$ isomer. The preferred loss of H over D from both of the intermediate product ions $C_3H_2D_4O^+$ and $C_3H_4D_2O^+$ [Reactions (9)–(12)] suggests that these ions have the cyclic structures X and XI. H or D loss occurs principally from the carbons adjacent to oxygen.



The results indicate a large deuterium isotope effect with H elimination approximately 2.5 times more favorable than D elimination.³⁷ Of the various $C_2H_4O^+$ structural isomers, the reactivity of only the $CH_2OCH_2^+$ ion VI is consistent with the present results. Structures IV and V would not be expected to react by CH_2^+ transfer. CH_2^+ transfer from $CH_2OCH_2^+$ to *n*-donor bases such as acetone,⁴ acetaldehyde,⁴ and phosphine⁸ is a facile process which is not observed for other $C_2H_4O^+$ structural isomers.⁴

The ICR studies indicate that at low conversion, where the relative ion abundance of $C_2H_5O^+$ is large and $C_3H_5O^+$ is not appreciable, the yield of the latter product is enhanced relative to the former by the addition of SF_6 . In trapped-ion experiments, where Reactions (1)–(3) have proceeded nearly to completion, the addition of SF_6 has a smaller effect on the product ratio. These results suggest that the collision gas efficiently deactivates vibrationally excited $(CH_2OCH_2^+)^*$ ions and that these “cooled” or deactivated ions react rapidly to produce $C_3H_5O^+$. This corresponds to an increase in the apparent rate of Reaction (3). Previous studies have shown that the reaction cross sections for ions in excited vibrational and electronic states can be considerably smaller than for ground state ions.^{13,14} In addition, it appears from the trapped-ion results that production of the $(CH_2OCH_2^+)^*$ ring-opened ion may be

level involves the release of considerable excess energy, approximately 29 ± 5 kcal/mole, to the internal modes of the acyclic ion VI. The results obtained from examination of the $C_3(H, D)_5O^+$ product distribution from a mixture of C_2H_4O with C_2D_4O are interpreted using the scheme of Reactions (15) and (16) (C_2H_4O alone). The ring-opened $(CH_2OCH_2^+)^*$ ion reacts by CH_2^+

somewhat increased [k_2 , Eq. (2)] by the collision of SF_6 with ethylene oxide.

The ICR data in Fig. 1 is in qualitative agreement with the time-resolved photoionization data of Fig. 7. Quantitative comparisons are not meaningful due to the poorly characterized distribution of states in the electron impact ionization process. When the extent of reaction is appreciable, the ratio of $C_2H_5O^+$ to $C_3H_5O^+$ reflects the relative populations of the $C_2H_4O^+$ vibrational levels. The trapped-ion ICR spectrum gives a ratio of 1.85, after correcting for the contribution of Reaction (5) to the $C_2H_5O^+$ abundance. This is not too different

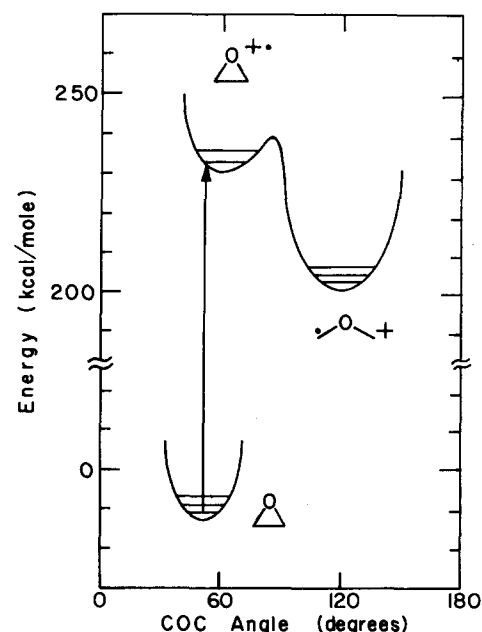


FIG. 9. Hypothetical energy surface for the isomerization of cyclic $C_2H_4O^+$ to acyclic $CH_2OCH_2^+$. The vibrational levels are for illustrative purposes only and are not indicative of a normal coordinate involving the COC angle. The isomerization to the open form involves CH_2 rotation in addition to changes in the COC angle. The energy scale is determined by the enthalpy of formation of the various species.

TABLE VII. Enthalpies of formation used in this work.

| Species | ΔH_f^a |
|--|----------------------|
| ethylene oxide | -12.58 ± 0.15^b |
| CO | -26.42 ± 0.04^b |
| CH ₄ | -17.895 ± 0.08^b |
| CH ₂ O | -25.95 ± 0.12^b |
| H· | 52.100 ± 0.001^b |
| C ₂ H ₄ O ⁺ (ethylene oxide) | 230.9 ± 0.5^c |
| C ₂ H ₃ O ⁺ | 203 ± 2^c |
| C ₂ H ₅ O ⁺ (protonated ethylene oxide) | 169 ± 1^d |
| CH ₃ ⁺ | 260 ± 1^e |
| CHO ⁺ | 195.6 ± 1.5^f |
| | 195.9 ± 1.0^g |
| CH ₂ OCH ₂ ⁺ | 201.9 ± 5^h |
| C ₃ H ₅ O ⁺ | 151 ± 3^h |
| C ₂ H ₃ O | 31 ± 3^h |

^aAll values in kcal/mole at 298 °K.

^bReference 48.

^cReference 19.

^dReference 8.

^eReference 38.

^fC. S. Matthews and P. Warneck, *J. Chem. Phys.* **51**, 854 (1969).

^gN. Jonathan, A. Morris, M. Okuda, and D. J. Smith, *J. Chem. Phys.* **55**, 3046 (1971).

^hThis work (see Appendix).

from the ratio of C₂H₅O⁺ to C₃H₅O⁺ obtained in the 1151 Å PIMS data [Fig. 7(b)] of 1.32, which is weighted by the relative populations of the $v=0$ and $v=1$ vibrational levels at 1151 Å (Table V). The PIMS data gives ratios of 6.7 and 0.32 for C₂H₄O⁺ initially in the $v=0$ and $v=1$ levels, respectively (Table VI). Thus, in the ICR experiment, electron impact ionization of ethylene oxide produces a substantial population of the C₂H₄O⁺ ions in the $v=1$ and higher vibrational levels. It is of interest that the effects of vibrational excitation remain evident in the ICR experiment. The collision time in the PIMS and ICR experiments are markedly different, being approximately 4×10^{-5} and 10^{-2} sec, respectively. The direct inference is that the radiative lifetime of the vibrational excitation is longer than 10^{-2} sec.

It is of interest to consider the conditions which cause the ring opening of C₂H₄O⁺ molecular ions to occur. While the ring opening of ethylene oxide and other three-membered rings has been considered in detail,⁴³⁻⁴⁵ we are not aware of such calculations for C₂H₄O⁺. The hypothetical energy surface presented in Fig. 9 summarizes the salient features of the rearrangement process. Although the ring-opened form is more stable than the cyclic C₂H₄O⁺ ion due to a favorable resonance interaction and release of internal strain (26.9 kcal/mole⁴⁶), all the present evidence indicates that rearrangement does not occur directly upon ionization at or near threshold. Consequently a barrier exists between the closed and open forms. The minimum energy pathway involves a simultaneous increase in the COC angle and rotation of the methylene groups into the COC plane. At small COC angles the energy surface of the acyclic CH₂OCH₂⁺ ion is quite repulsive because of the unfavorable H···H interaction. It was our expectation that activation of cyclic C₂H₄O⁺ ions in energetic collisions (Sec. III. B) would cause the formation

of (CH₂OCH₂)⁺ by converting translational energy into external excitation. However, the results show that rather than promote the collision-induced isomerization, the C₂H₄O⁺ molecular ion dissociates to CHO⁺ and C₂H₃O⁺ ions by Reactions (7) and (8). A specific intimate collision complex is probably excluded in the isomerization reaction because there is very little isotopic scrambling, products such as (C₂H₂D₂O⁺)⁺ are not observed in the C₂H₄O–C₂D₄O mixture, and there is no significant charge transfer. This contrasts markedly with the behavior exhibited by ethylene, where both isotopic scrambling and charge transfer serve as diagnostics for the characterization of the intermediate complex.¹⁴ It appears that interaction of C₂H₄O⁺ with C₂H₄O involves a rather subtle modification of the potential energy surface which facilitates the ring opening process. A theoretical study of the C₂H₄O⁺ surface might possibly clarify the isomerization process.

APPENDIX—SOURCES OF THERMOCHEMICAL DATA

The enthalpies of formation of several key ions and neutrals considered in this study are presented in Table VII. The heat of formation of the C₂H₄O⁺ isomer with structure VI was computed by assuming that $D[\text{H}-\text{CH}_2\text{OCH}_2^+] = D[\text{H}-\text{CH}_2\text{OH}] = 92 \pm 2$ kcal/mole.⁴⁷ $\Delta H_f(\text{C}_3\text{H}_5\text{O}^+)$ was calculated by taking the average hydride affinity, $D[\text{R}^+-\text{H}^-]$, of the two ethers (CH₃)₂O and C₂H₅OCH₃,^{48,49} to give the three ions CH₃OCH₂⁺, CH₃CHOCH₃⁺, CH₃CH₂OCH₂⁺.³⁸ From $D[\text{R}^+-\text{H}^-] = 236 \pm 3$ kcal/mole and $\Delta H_f(\text{CH}_3\text{OCHCH}_2) = 27.1 \pm 1$ kcal/mole,³⁸ $\Delta H_f(\text{C}_3\text{H}_5\text{O}^+) = 151 \pm 3$ kcal/mole was estimated.

*This research was supported in part by the United States Energy Research and Development Administration under Grant No. AT(04-3) 767-8 awarded to J. L. Beauchamp and presents one phase of research carried out at the Jet Propulsion Laboratory, California Institute of Technology under Contract No. NAS7-100, sponsored by the National Aeronautics and Space Administration. The PIMS instrumentation was made possible by a grant from the President's Fund of the California Institute of Technology.

[†]NASA-JPL Postdoctoral Research Fellow, 1972–1973. Permanent address: Department of Chemistry, University of Illinois, Chicago Circle, IL.

[‡]Sherman Fairchild Research Fellow, 1973. Permanent address: Department of Chemistry, University of Minnesota, Minneapolis, MN 55455.

[§]Camille and Henry Dreyfus Teacher-Scholar, 1971–1976. Author to whom correspondence should be addressed.

^{||}Contribution No. 5196.

¹H. Pritchard and A. G. Harrison, *J. Chem. Phys.* **48**, 5623 (1968).

²M. Kumakura and T. Sugiura, in *Recent Developments in Mass Spectroscopy*, edited by K. Ogata and T. Hayakawa (University Park, Baltimore, 1970), p. 988.

³A. Giardini-Guidoni, A. Mele, R. Platania, and F. Zocchi, *J. Chem. Soc. Faraday II* **71**, 351 (1975).

⁴A. S. Blair and A. G. Harrison, *Can. J. Chem.* **51**, 703 (1973).

⁵B. G. Keyes and A. G. Harrison, *Org. Mass Spectrom.* **9**, 221 (1974).

⁶J. L. Beauchamp and R. C. Dunbar, *J. Am. Chem. Soc.* **92**, 1477 (1970).

⁷M. T. Bowers and P. R. Kemper, *J. Am. Chem. Soc.* **93**, 5352 (1971).

⁸R. H. Staley, R. R. Corderman, M. S. Foster, and J. L.

- Beauchamp, *J. Am. Chem. Soc.* **96**, 1260 (1974).
- ⁹D. W. Turner, C. Baker, A. D. Baker, and C. R. Brundle, *Molecular Photoelectron Spectroscopy* (Wiley-Interscience, London, 1970).
- ¹⁰M. T. Bowers, D. H. Aue, and D. D. Elleman, *J. Am. Chem. Soc.* **94**, 4255 (1972) and references contained therein.
- ¹¹T. B. McMahon and J. L. Beauchamp, *Rev. Sci. Instrum.* **43**, 509 (1972).
- ¹²S. E. Buttrill, *J. Chem. Phys.* **61**, 619 (1974).
- ¹³J. M. Ajello, W. T. Huntress, A. L. Lane, P. R. LeBreton, and A. D. Williamson, *J. Chem. Phys.* **60**, 1211 (1974) and J. M. Ajello, K. D. Pang, and K. Monahan, *J. Chem. Phys.* **61**, 3152 (1974).
- ¹⁴P. R. LeBreton, A. D. Williamson, J. L. Beauchamp, and W. T. Huntress, *J. Chem. Phys.* **62**, 1623 (1975).
- ¹⁵S. E. Buttrill, J. K. Kim, W. T. Huntress, P. R. LeBreton, and A. D. Williamson, *J. Chem. Phys.* **61**, 2122 (1974).
- ¹⁶H. Basch, M. B. Robin, N. A. Kuebler, C. Baker, and D. W. Turner, *J. Chem. Phys.* **51**, 52 (1969).
- ¹⁷A. Schweig and W. Thiel, *Chem. Phys. Lett.* **21**, 541 (1973).
- ¹⁸A. W. Potts, T. A. Williams, and W. C. Price, *Faraday Discuss.* **54**, 104 (1972).
- ¹⁹R. Krässig, D. Reinke, and H. Baumgärtel, *Ber. Bunsenges. Phys. Chem.* **78**, 425 (1974).
- ²⁰A. Lowrey III and K. Watanabe, *J. Chem. Phys.* **28**, 208 (1958).
- ²¹H. Hurler, M. G. Inghram, and J. D. Morrison, *J. Chem. Phys.* **28**, 76 (1958).
- ²²M. S. Foster, A. D. Williamson, and J. L. Beauchamp, *Int. J. Mass Spectrom. Ion Phys.* **15**, 429 (1974).
- ²³R. Allison, J. Burns, and A. J. Tuzzolino, *J. Opt. Soc. Am.* **54**, 747 (1964).
- ²⁴J. L. Beauchamp, *Ann. Rev. Phys. Chem.* **22**, 527 (1971).
- ²⁵B. S. Freiser, T. B. McMahon, and J. L. Beauchamp, *Int. J. Mass Spectrom. Ion Phys.* **12**, 249 (1973).
- ²⁶S. E. Buttrill, *Proc. Ann. Conf. Mass Spectrom. All. Topics 19th, Atlanta, GA., 1971*, p. 349; W. T. Huntress, Jr., *J. Chem. Phys.* **56**, 5111 (1972).
- ²⁷E. J. Gallegos and R. W. Kiser, *J. Am. Chem. Soc.* **83**, 773 (1961).
- ²⁸J. A. Gilpin and F. W. McLafferty, *Anal. Chem.* **29**, 990 (1957).
- ²⁹J. H. Beynon, in *Advances in Mass Spectrometry*, edited by J. D. Waldron, (Pergamon, London, 1959), p. 328.
- ³⁰Pressures were measured as described by R. J. Blint, T. B. McMahon and J. L. Beauchamp, *J. Am. Chem. Soc.* **96**, 1269 (1974).
- ³¹G. Gioumousis and D. P. Stevenson, *J. Chem. Phys.* **29**, 294 (1958).
- ³²The value of α used was 4.43×10^{-24} cm³ from K. L. Ramaswamy, *Proc. Indian Acad. Sci. Sec. A* **4**, 675 (1936).
- ³³S. K. Gupta, E. G. Jones, A. G. Harrison, and J. J. Myher, *Can. J. Chem.* **45**, 3107 (1967).
- ³⁴S. E. Buttrill, *J. Chem. Phys.*, **58**, 656 (1973).
- ³⁵T. Su and M. T. Bowers, *Int. J. Mass Spectrom. Ion Phys.* **12**, 347 (1973).
- ³⁶A. Giardini-Guidoni, R. Platania, and F. Zocchi, *Int. J. Mass Spectrom. Ion Phys.* **13**, 453 (1974).
- ³⁷Product ions of mass 58, 60, 62, and 64 were also observed in low abundance (<7% of total). These may be formulated as C₃H_{6-n}D_nO⁺ ($n=0, 2, 4, 6$) ions which result from CH₂(CD₂) transfer to small amounts of acetaldehyde and acetaldehyde-d₄ which are produced in small amounts in the ICR spectrometer by isomerization of ethylene oxide. In addition, a small fraction of the C₃H_{6-n}D_nO⁺ ($n=0, 2, 4, 6$) intermediate product ions may have insufficient energy to eliminate H or D via unimolecular decomposition.
- ³⁸J. L. Franklin, J. G. Dillard, N. M. Rosenstock, J. T. Herron, K. Draxl, and F. H. Field, *Natl. Stand. Res. Data Ser. Natl. Bur. Stand.* **26** (1969).
- ³⁹P. G. Miasek and A. G. Harrison, *J. Am. Chem. Soc.* **97**, 714 (1975).
- ⁴⁰W. J. Potts, *Spectrochim. Acta* **24**, 511 (1965).
- ⁴¹R. C. Lord and B. Nolin, *J. Chem. Phys.* **24**, 656 (1956).
- ⁴²S. Evans, P. J. Joachim, A. F. Orchard, and D. W. Turner, *Int. J. Mass Spectrom. Ion Phys.* **9**, 41 (1972).
- ⁴³R. Bonaccorsi, E. Scrocco, and J. Tomasi, *J. Chem. Phys.* **52**, 5270 (1970).
- ⁴⁴E. F. Hayes, *J. Chem. Phys.* **51**, 4787 (1969).
- ⁴⁵P. Mezey, R. E. Kari, A. S. Denes, I. G. Csizmadia, R. K. Gosavi, and O. P. Strausz, *Theor. Chim. Acta (Berlin)* **36**, 329 (1975).
- ⁴⁶S. W. Benson, *Thermochemical Kinetics* (Wiley, New York, 1968).
- ⁴⁷F. R. Cruickshank and S. W. Benson, *J. Phys. Chem.* **73**, 733 (1969).
- ⁴⁸J. D. Cox and G. Pilcher, *Thermochemistry of Organic and Organometallic Compounds* (Academic, London, 1970).
- ⁴⁹A. A. Planckaert, J. Doucet, and C. Sandorfy, *J. Chem. Phys.* **60**, 4846 (1974).